Towards true 3-dimensional BCC colloidal crystals with controlled lattice orientation

Nina V. Dziomkina, Mark A. Hempenius, G. Julius Vancso*

Materials Science and Technology of Polymers, MESA+ Institute for Nanotechnology, University of Twente, P.O. Box 217, 7500 AE Enschede, The Netherlands

ARTICLE INFO

ABSTRACT

A fabrication method of colloidal crystals possessing the BCC crystal structure is described. BCC colloidal crystals with a thickness of up to seven colloidal layers were grown in the direction of the (100) crystal plane. Defect free colloidal crystals with a homogeneous surface coverage were obtained over a surface area of several square millimeters. Quality and thickness of grown colloidal crystals were controlled by a set of deposition parameters such as deposition voltage, deposition time, and concentration of colloidal particles in the colloidal suspension, colloid surface charge density and withdrawal speed of electrodes out of the suspension. Optimal deposition parameters leading to a controlled BCC colloidal crystal growth were established.

© 2009 Elsevier Ltd. All rights reserved.

1. Introduction

Colloidal crystals have recently found use in a wide range of applications such as in optics [1], as chemical sensors [2] and in data storage [3]. In optics, colloidal crystals become particularly important as they can be used as a basis for photonic crystals. Photonic crystals [4] are 3-dimensional periodic structures that are able to block light propagation in one or more directions. The direction of light propagation in photonic crystals is highly dependent on the crystal structure. It was predicted that colloidal crystals with a diamond structure are able to block the light in all directions [5], therefore, opening many possibilities to guide light by defect structure control. Fabrication of colloidal crystals with the diamond structure by self-assembly of colloidal particles is still impossible due to a low colloidal packing fraction of 0.34. The structure that is usually obtained by self-assembly of colloidal particles on a flat substrate is a close-packed structure such as face-centered cubic (FCC) with a packing density of 0.74, stacked in the direction of the close-packed (111) plane [6,7]. The body-centered cubic (BCC) structure possesses a packing density of 0.68, only slightly lower than that of the FCC, but it is already a problem to fabricate such a structure in a controlled way. Realization of the controlled growth of a BCC colloidal crystal structure will allow one to make a step towards the non-close-packed diamond structure.

The method of template-directed colloidal crystallization has already been demonstrated to influence colloidal crystal orientation of close-packed crystals [8–10], the size of colloidal crystals [11,12] and to a certain degree the crystal structure [13,14]. Furthermore, the pattern of the surface predetermines the location of the colloidal crystal on the surface which is an important aspect for planar integration technology.

The application of an electric field accelerates the growth of the 3D colloidal crystals on the flat electrode surface [15]. Careful adjustment of colloidal concentration and electric field strength leads to the formation of various non-close-packed crystal structures [16]. These different crystal structures were observed using a confocal microscope directly in the colloidal suspension but not as solid crystals (a free-standing colloidal crystal). Capillary forces, acting between colloidal particles, simply destroy non-close-packed colloidal crystals when a sample is withdrawn from the colloidal suspension.

In this paper, the fabrication of free-standing colloidal crystals with a BCC crystal structure is discussed. The method of electrophoretic deposition of charged polymer colloidal particles onto patterned electrode substrates was applied [17]. This method combines the advantages of the methods mentioned earlier: application of the electric field gives the directionality to the colloidal crystal growth and defines the speed of the colloidal deposition, and the patterned electrode surface induces the colloidal crystal structure. The quality and thickness of grown BCC colloidal crystals in this case are highly dependent on the various deposition parameters such as deposition voltage, deposition time,

---

* Corresponding author. Tel.: +31 534892974; fax: +31 534893823.
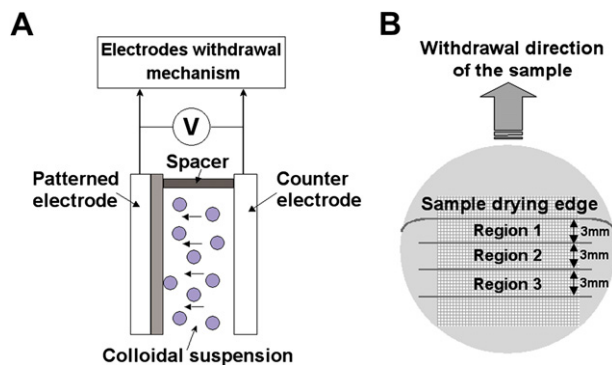 E-mail address: g.j.vancso@utwente.nl (G.J. Vancso).

Fig. 1. A) Schematic illustration of the electrophoretic deposition set-up; B) Schematic representation of the patterned electrode showing the various regions used in SEM analysis.

concentration of colloidal particles in suspension, surface charge density of colloidal particles and withdrawal speed of the electrodes out of the colloidal suspension after the electrophoretic deposition. The influence of the deposition parameters on the BCC colloidal crystal growth is the main subject of this paper.

2. Results and discussion

Colloidal crystals were fabricated using an electrophoretic deposition set-up as shown in Fig. 1. This figure also shows a schematic representation of the patterned electrode and the various regions used for SEM analysis. Effective surface coverage as an

equivalent value of the average number of colloidal layers was calculated from SEM images over three regions. Homogeneous surface coverage was observed in regions 2 and 3. Surface coverages reported here were obtained from region 2.

Deposition results at different applied voltages are presented in Fig. 2. Colloidal particles with a surface charge density of 16.2 μC/cm^2 and a colloid concentration of 0.5 vol% were deposited on a patterned electrode surface for 1 min and finally withdrawn from the colloidal suspension with a speed of 0.04 mm/s. An increase in the applied voltage leads to an increase in the surface coverage. A significant growth of colloidal crystals was detected above a certain voltage, called the threshold voltage. The value of the threshold voltage was determined as 3.0 V. Therefore, for colloidal crystal growth, values of applied voltages above the threshold voltage were used.

As it is clearly seen in the SEM images, thick colloidal crystals with polycrystalline domains were obtained with packing features that do not correspond to the electrode pattern. The polycrystalline structure of the colloidal crystals can be a result of high concentration and/or the relatively low withdrawal speed of electrodes out of the colloidal suspension. In the first case, colloidal particles do not have enough time to rearrange to accommodate packing in accordance to the electrode pattern because they are too many. In the second case, colloidal particles under the influence of the high capillary force get rearranged and become tightly packed. Therefore, by adjusting colloidal concentration and withdrawal speed of electrodes, ordering of colloidal particles into a BCC structure can be induced.

The results of the deposition of colloidal particles at different concentrations such as 0.175, 0.2 and 0.5 vol% are presented in
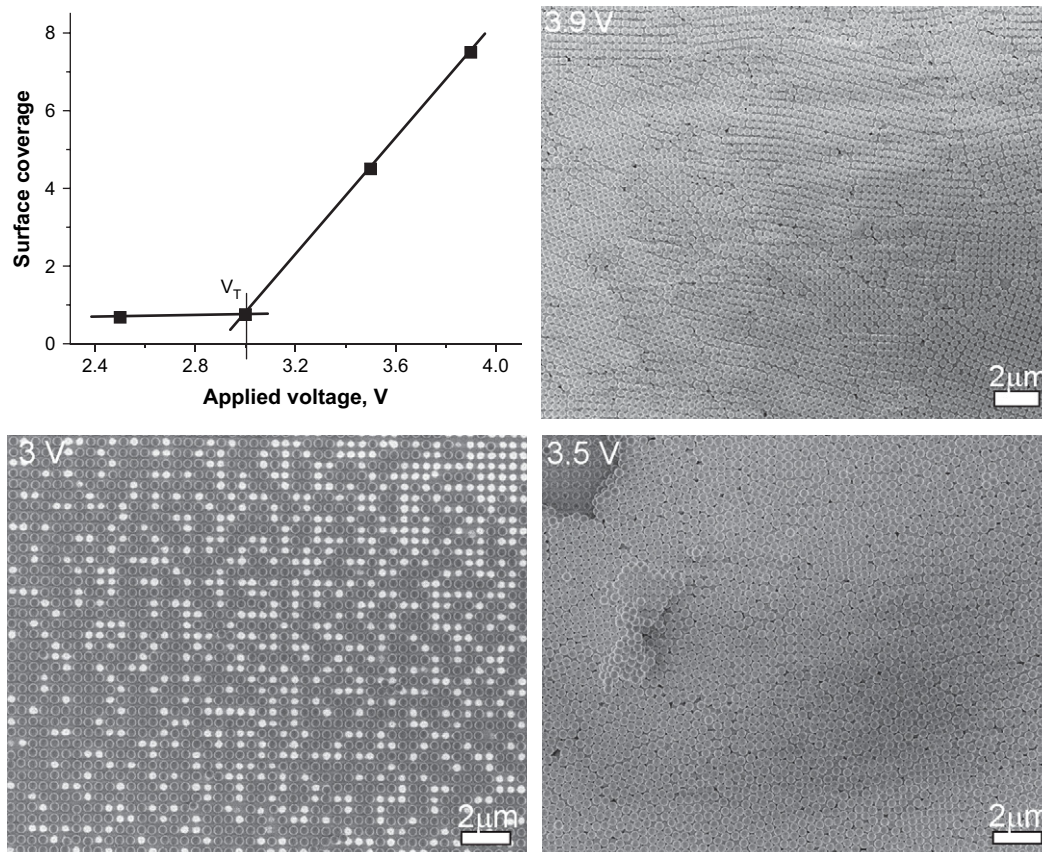

Fig. 2. Surface coverage of colloidal particles versus deposition voltage. The threshold voltage was determined to be 3.0 V. SEM images show a top view of the grown colloidal crystals.

Fig. 3. Colloidal particles with a surface charge density of 16.2 μC/cm^2 were deposited for 9 min at 3.5 V and then the electrodes were withdrawn from the colloidal suspension with a speed of 0.08 mm/s. Surface coverage was calculated over region 2, Fig. 1B. For the colloidal suspension with a concentration of 0.5 vol%, an increase in withdrawal speed from 0.04 mm/s (Fig. 2) to 0.08 mm/s (Fig. 3) led to a decrease in the number of deposited colloidal layers. In addition, an increase in withdrawal speed led to an improvement in the colloidal particle ordering, where relatively large BCC colloidal crystal domains with a (100) crystal plane parallel to the electrode surface are easily recognized among hexagonal close-packed domains.

A decrease in colloidal concentration from 0.5 vol% to 0.2 vol% and 0.175 vol% improved the ordering of colloidal particles substantially, as the top layer of colloidal crystals in SEM images (Fig. 3) completely replicated the electrode pattern over almost the full electrode surface area of several square millimeters. The difference in the quality of colloidal layers grown from colloidal suspensions with 0.2 vol% and 0.175 vol% is very small, but the difference in the number of deposited colloidal layers is significant. Therefore, colloidal depositions in a colloidal suspension of 0.2 vol% were preferred for further electrophoretic depositions.

The influence of electrode withdrawal speed out of the colloidal suspension on the colloidal crystal ordering is presented in Fig. 4. Colloidal particles with a surface charge density of 16.2 μC/cm^2 were deposited onto a patterned electrode within 9 min at 3.5 V and withdrawn out of the colloidal suspension with a concentration of 0.2 vol%. Surface coverage was calculated over region 2, Fig. 1B.

The influence of withdrawal speed on the colloidal ordering was already mentioned when colloidal depositions in colloidal suspensions of 0.5 vol% were discussed. The same effect was observed for a colloidal concentration of 0.2 vol%. Increase in withdrawal speed decreased the number of deposited colloidal layers. At the same time, the quality of colloidal crystals increased when the withdrawal speed increased from 0.05 mm/s to 0.08 mm/s and 0.1 mm/s. At 0.05 mm/s, relatively large colloidal crystal domains with a BCC crystal structure were observed among hexagonally close-packed domains. The difference in quality of colloidal crystals grown, when withdrawal speeds of 0.08 mm/s and 0.1 mm/s were maintained, was rather small. On the contrary, the thickness of colloidal crystals differed remarkably (Fig. 4), therefore, a withdrawal speed of 0.08 mm/s was found to be optimal for BCC colloidal crystal growth with the (100) plane parallel to the electrode surface. Homogeneous surface coverage of BCC colloidal crystals was determined on the electrode surface area over several square millimeters.

Surface charge densities of colloidal particles influence the colloidal ordering on patterned surfaces. Colloidal particles possessing different surface charge densities of 16.2 μC/cm^2 and 26.5 μC/cm^2 were deposited for 9 min in a colloidal suspension with a colloid concentration of 0.2 vol% on a patterned electrode. A deposition voltage of 3.5 V and withdrawal speed of 0.08 mm/s were applied. Increase in surface charge density led to an increase in the number of deposited colloidal layers. As a result, polycrystalline close-packed colloidal crystals with various orientations in plane were obtained that did not correspond to the electrode pattern, Fig. 5B. On the contrary, for low charge densities of 16.2 μC/cm^2, significantly lower numbers of colloidal layers were obtained, but colloidal crystal structures grown corresponded very well to the electrode pattern and covered electrode areas over several square millimeters, Fig. 5A.
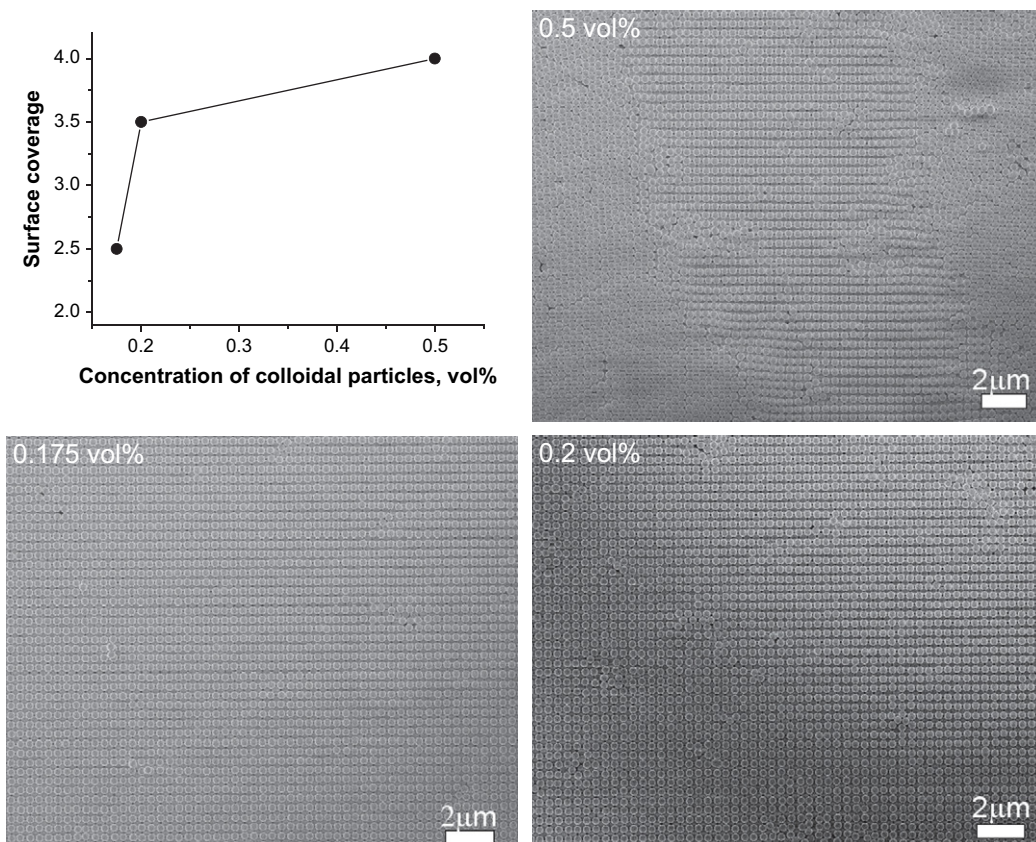

Fig. 3. Surface coverage versus colloidal particle concentration. SEM images show a top view of colloidal crystals grown at different colloidal concentrations. The displayed structures consist of 3 layers for the concentrations 0.175 and 0.2 vol% and of 4 layers for 0.5 vol%.
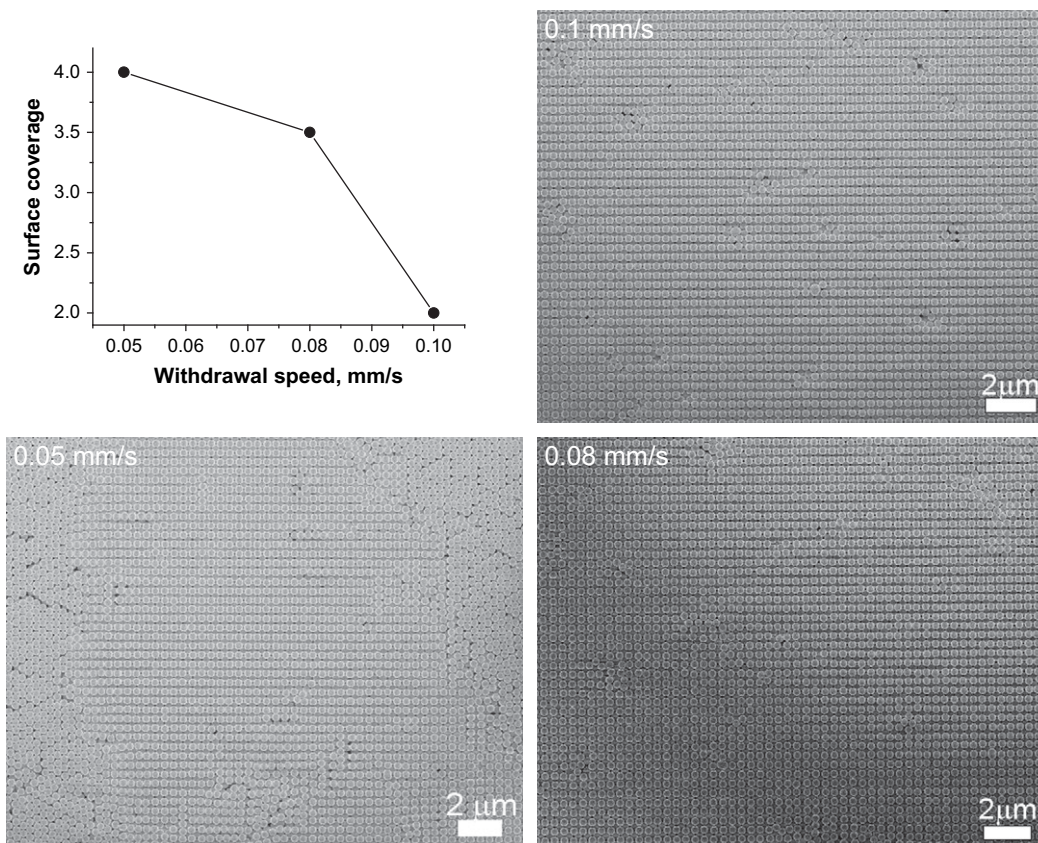
Fig. 4. Surface coverage versus withdrawal speed of the electrodes from the colloidal suspension. SEM images show top views of colloidal crystals grown at different withdrawal speeds. The displayed structures have a thickness of 4 layers for withdrawal speeds of 0.05 mm/s, 3 layers at 0.08 mm/s and 2 layers at 1 mm/s.

At short deposition times (several minutes), highly charged colloids with a surface charge density of 26.5 $\mu C/cm^2$ were arranged as well according to the electrode surface pattern, forming colloidal crystals possessing a BCC structure with a thickness of several colloidal layers grown over large surface areas. Despite the fact that at shorter deposition times, colloidal crystals can also be grown from colloidal particles with a surface charge density of 26.5 $\mu C/cm^2$, control over the colloidal deposition was easier when colloidal particles with a low surface charge density were used. Therefore, colloidal particles with a surface charge density of 16.2 $\mu C/cm^2$ were preferred for colloidal depositions.

Finally, the growth of colloidal crystals as a function of deposition time was followed, applying the most suitable deposition parameters discussed above. Colloidal particles with a surface charge density of 16.2 $\mu C/cm^2$ were deposited at different deposition times in the colloidal suspension with a concentration of 0.2 vol% at 3.5 V and a withdrawal speed of 0.08 mm/s, Fig. 6.

Increase in the deposition time showed a linear increase in colloidal surface coverage. Examples of colloidal crystals with different thicknesses are presented in the SEM images, Fig. 6a–e. Such colloidal crystals covered large electrode areas of several square millimeters. The thickness of the colloidal crystals could be
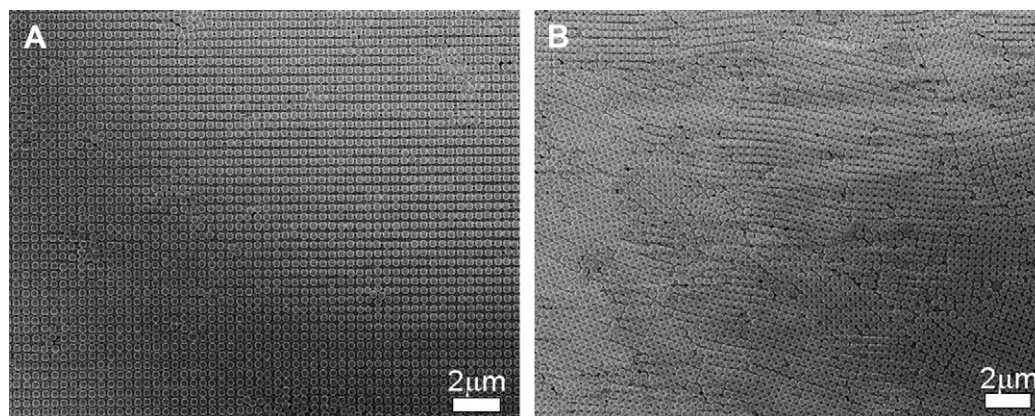

Fig. 5. SEM images (top view) of colloidal crystals grown with colloidal particles possessing different surface charge densities A) 16.2 $\mu C/cm^2$ and B) 26.5 $\mu C/cm^2$. For a particle surface charge density of 16.2 $\mu C/cm^2$ a thickness of 3 layers was obtained and for 26.5 $\mu C/cm^2$ more than 6 layers.
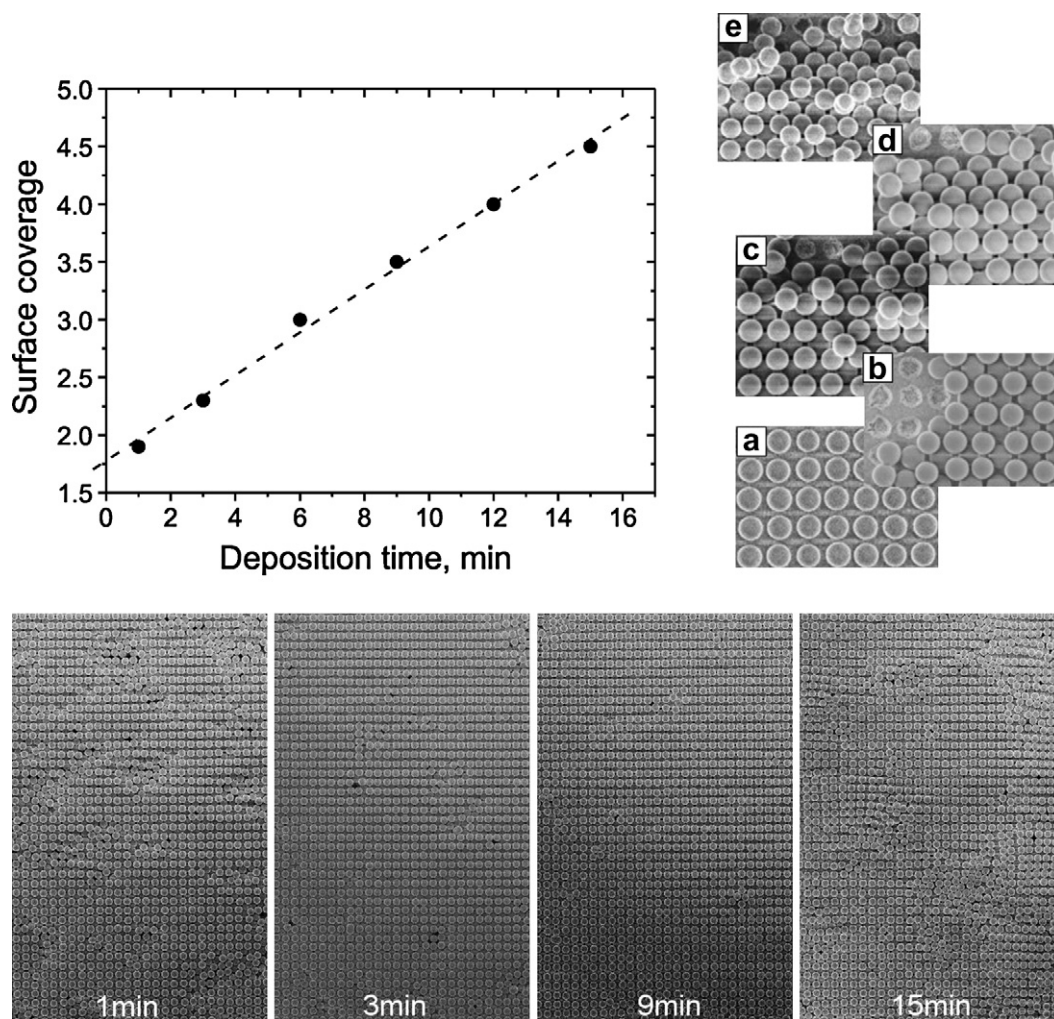
Fig. 6. Surface coverage versus deposition time calculated over the region 2 ([Surface coverage, layers] = 1.78 + 0.19 · [deposition time, min]), (top left corner). SEM images of crystals with various thicknesses (top right corner): a) 1 layer, b) 2 layers, c) 3 layers, d) 4 layers and e) 5 layers. These SEM images demonstrate how the colloidal crystal thicknesses were determined. SEM images in the bottom represent top views of colloidal crystals grown at different deposition times. On the SEM images for 1 min the crystal thickness is almost 2 layers, for 3 min – 2 layers, for 9 min – 3 layers and for 15 min – 4 layers.

accurately controlled at fixed deposition parameters and was rather reproducible. Top layers of colloidal crystals, whose values of surface coverage are presented in the graph, are shown in the SEM images placed at the bottom of Fig. 6. Large, almost defect free colloidal crystals were grown up to a deposition time of 15 min. At the deposition time of 15 min, crystal defects were observed,

destroying the colloidal crystal homogeneity. Upon increasing the deposition time further to 20 min, polycrystalline close-packed domains and no BCC colloidal crystal domains were observed. Therefore, using this method, colloidal crystals possessing a BCC crystal structure oriented in the direction of the (100) plane could be grown with a thickness of up to five colloidal layers.
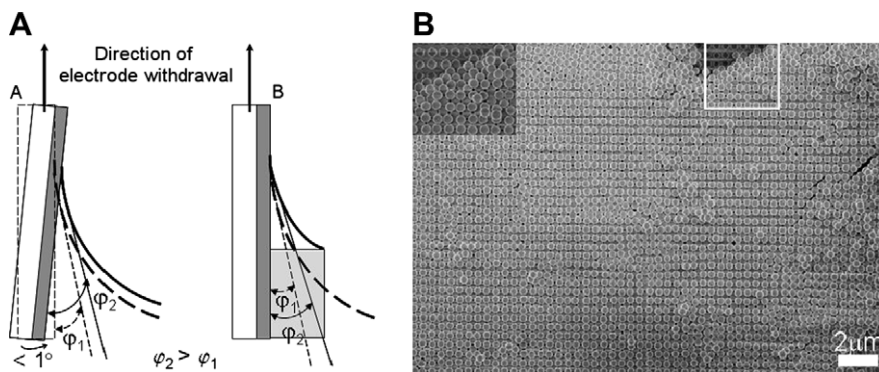

Fig. 7. A) Two types of meniscus modification: A) by tilting the sample in relation to the colloidal suspension or B) by introducing obstacles of certain thickness. B) SEM image of colloidal crystals with a thickness of 6 layers grown by the tilt method. Deposition voltage was 3.5 V, deposition time 15 min, colloidal concentration 0.175 vol%, colloidal surface charge density 16.2 μC/cm² and withdrawal speed 0.08 mm/s.
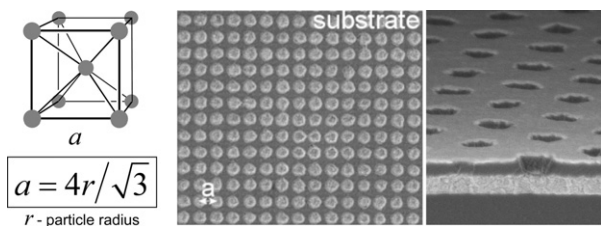
Fig. 8. Schematic illustration of BCC structure (left), in the calculation of the pattern periodicity it is considered that the colloidal particles are touching at the diagonal; SEM image of the patterned electrode surface with a periodicity equal to the distance between colloids in the (100) plane: top view (middle) and side view (right).

In order to increase the number of layers of colloidal crystals further, we varied the meniscus shape of the colloidal suspension between the electrodes, Fig. 7A. The meniscus can be induced by several methods: 1) by changing the tilt angle of electrodes with respect to the colloidal suspension by a few degrees or 2) to use artificial obstacles for the colloidal suspension of different thicknesses. We tried both methods and we obtained the same results. The disadvantage of the second method is that not the whole electrode surface takes part in the colloidal deposition and thickness control of colloidal crystal growth has to be realized by the precise level of electrode submersion in the colloidal suspension. The first method is easier to put in practice, as only a tilt angle has to be fixed during the colloidal deposition. As a result, by changing the tilt angle by around 1–2°, colloidal crystals possessing a BCC crystal structure and a thickness of up to seven colloidal layers were achieved. Colloidal crystals with a BCC crystal structure and with a thickness of six colloidal layers are presented in Fig. 7B.

Another very important parameter that influences the quality of the grown colloidal crystals is the quality of the patterned electrode surface. Laser interference lithography (LIL) was used to generate the highly periodic structure of the electrode surface. The size of the individual electrode features (hole in the SiO_2 layer) was in the order of 200 nm. This is a rather small distance and therefore the quality of the patterned layer is highly dependent on the lithographic steps. Improvements of the quality of the patterned electrode layer can further increase the quality of the grown colloidal crystals. An example of a final electrode with a square pattern is shown in Fig. 8. The electrode pattern was chosen in accordance with the (100) plane of a BCC structure and generated using LIL over an electrode surface area of 1.5 × 1.5 cm. Pattern periodicity equals to the distance between neighboring colloids in the (100) plane. Fig. 8 presents a top view (middle) and a side view (right) of the periodic array of holes in the electrode surface.

3. Conclusion

In summary, a fabrication method of colloidal crystals possessing the BCC crystal structure is discussed. BCC colloidal crystals with a thickness of up to seven colloidal layers were grown in the direction of the (100) crystal plane. Defect free colloidal crystals with a homogeneous surface coverage were obtained over a surface area of several square millimeters. Quality and thickness of grown colloidal crystals were controlled by a set of deposition parameters such as deposition voltage, deposition time, and concentration of colloidal particles in the colloidal suspension, colloid surface charge density and withdrawal speed of electrodes out of the suspension. A threshold voltage of 3.0 V was determined, beyond which a significant crystal growth was observed. Optimal deposition parameters that lead to a controlled BCC colloidal crystal growth were found such as an applied voltage of 3.5 V, colloidal volume

fraction of 0.2 vol%, colloid surface charge density of 16.2 μC/cm^2 and a withdrawal speed of 0.08 mm/s.

4. Experimental section

4.1. Electrode patterning

Electrodes consisting of 1 inch float glass disks with a 100 nm conductive ITO layer were supplied by Ssens bv, The Netherlands and were used as received. A dielectric layer of SiO_2 was deposited on the ITO electrodes in an e-gun evaporator (Balzers BAK 600). The thickness of the dielectric layer was 100 nm. The surface patterns used were generated in a positive photoresist (Olin 907/12) layer with a thickness of 200 nm by laser interference lithography (LIL). LIL exposures were performed with an Azure™ solid-state laser at a wavelength of 266 nm. The photoresist pattern was further transferred by the so-called "lift-off" process into the SiO_2 dielectric layer to yield e.g. a periodic array of holes. An example of a final electrode with a square pattern is shown in Fig. 8. The whole patterning procedure was explained in detail in a previous publication [17]. The electrode pattern was chosen in accordance with the (100) plane of a BCC structure (Fig. 8) and generated using LIL over an electrode surface area of 1.5 × 1.5 cm. Pattern periodicity equals to the distance between neighboring colloids in the (100) plane.

4.2. Synthesis of polymer colloidal microparticles

Negatively charged polystyrene colloidal particles were synthesized by emulsifier-free emulsion polymerization [18]. Size and polydispersity of the polystyrene colloids were determined from SEM images. The size variation from the mean diameter of the colloids synthesized was less than 4%. Surface charge density was controlled via the copolymerization of styrene with sodium styrene sulfonate around previously prepared polystyrene colloids [19]. Surface charge density was determined by conductometric titration. Polystyrene colloidal particles were centrifuged several times at 17 000 rpm and redispersed in Milli-Q water, then passed through an ion-exchange column filled with Amberlite IR-120(plus) (Aldrich) several times and finally dialyzed for several days using a Spectra/Por membrane (molar mass cutoff of 12–14 000 g mol^{-1}, Spectrum Laboratories) until the conductivity of the Milli-Q water used became constant. Subsequently, the colloids were titrated with 0.01 N NaOH.

4.3. Deposition of colloidal particles

The cell for electrophoresis is schematically illustrated in Fig. 1A. Two glass/ITO electrodes were separated from each other with a 1 mm thick Teflon spacer. One of the electrodes was patterned as described above. The cell was immersed into a colloidal suspension, perpendicular to the suspension surface. In the colloidal suspension, polymer colloidal particles were redistributed in a mixture of ethanol and water in the proportion of 80:20 (v:v). Colloidal volume fractions of 0.175, 0.2 and 0.5 vol% were used. Negatively charged polystyrene colloidal particles with a mean diameter of 330 nm and surface charge densities of 16.2 and 26.5 μC/cm^2 were compared. When an electric field was applied, the charged polymer colloidal particles moved to the oppositely charged patterned electrode and were deposited on its surface. After a fixed deposition time, the cell was withdrawn with a certain constant speed from the colloidal suspension. The patterned electrode was left for several minutes to dry without turning off the applied voltage. Patterned electrodes with deposited colloids were marked in three regions (each region was 3 mm high) starting from the drying edge.

These three marked regions of the sample are shown schematically in Fig. 1B. The distribution of the colloidal particles on the electrodes was studied by a high-resolution scanning electron microscope (LEO 1550 FEF HR-SEM). Effective surface coverage as an equivalent value of the average number of colloidal layers was calculated from SEM images over three regions. Homogeneous surface coverage was observed in regions 2 and 3. Surface coverages reported here were obtained from region 2.

Acknowledgements

References

[1] Colvin VL. MRS Bull 2001;26:637.
[2] Holtz JH, Asher SA. Nature 1997;389:829.
[3] Gourevich I, Pham H, Jonkman JEN, Kumacheva E. Chem Mater 2004;16:1472.
[4] (a) Joannopoulos JD, Meade RD, Winn JN. In: Photonic crystals: molding the flow of light. Princeton, NJ: Princeton University Press; 1996;
(b) Paquet C, Kumacheva E. Materials Today 2008;11:48.
[5] Ho KM, Chan CT, Soukoulis CM. Phys Rev Lett 1990;65:3152.
[6] Dimitrov AS, Nagayama K. Langmuir 1996;12:1303.
[7] Jiang P, Bertone JF, Hwang KS, Colvin VL. Chem Mater 1999;11:2132.
[8] van Blaaderen A, Ruel R, Wiltzius P. Nature 1997;385:321.
[9] Yin Y, Xia Y. Adv Mater 2002;14:605.
[10] Dziomkina NV, Hempenius MA, Vancso GJ. Proc SPIE 2005;5931:59310Z.
[11] Yang SM, Ozin GA. Chem Commun 2000:2507.
[12] Park SH, Qin D, Xia Y. Adv Mater 1998;10:1028.
[13] Hoogenboom JP, Retif C, de Bres E, van de Boer M, van Langen-Suurling AK, Romijn J, et al. Nano Lett 2004;4:205.
[14] Yi D-K, Seo E-M, Kim D-Y. Appl Phys Lett 2002;80:225.
[15] Holgado M, Garcia-Santamaria F, Blanco A, Ibisate M, Cintas A, Miguiz H, et al. Langmuir 1999;15:4701.
[16] (a) Yethiraj A, van Blaaderen A. Nature 2003;421:513. For other recent colloidal crystal fabrication methods see for instance:
(b) Hartsuiker A, Vos WL. Langmuir 2008;24:4670;
(c) Wang D, Möhwald H. Adv Mater 2004;16:244;
(d) Varghese B, Cheong FC, Sindhu S, Yu T, Lim C-T, Valiyaveettil S, et al. Langmuir 2006;22:8248;
(e) Mukhopadhyay R, Al-Hanbali O, Pillai S, Hemmersam AG, Meyer RL, Hunter AC, et al. J Am Chem Soc 2007;129:13390;
(f) Hur J, Won Y-Y. Soft Matter 2008;4:1261.
[17] Dziomkina NV, Hempenius MA, Vancso GJ. Adv Mater 2005;17:237.
[18] (a) Goodwin JW, Hearn J, Ho CC, Ottewill RH. Colloid Polym Sci 1974;252:464;
(b) Dziomkina NV, Hempenius MA, Vancso GJ. Eur Polym J 2006;42:81;
(c) Oláh A, Hempenius MA, Vancso GJ. Eur Polym J 2004;40:763.
[19] Kim JH, Chainey M, El-Aasser MS, Vanderhoff JW. J Polym Sci Part A 1989;27:3187.